POROSITY CHARACTERIZATION OF MICROPOROUS SMALL CERAMIC COMPONENTS

Akshaya Jena, Krishna Gupta
Porous Materials, Inc., 20 Dutch Mill Road
Ithaca, NY 14850
and
Partho Sarkar, Hongsang Rho
Alberta Research Council, 250 Karl Clark Road
Edmonton, Canada R6N 1E4

ABSTRACT

Capillary flow porometry with modifications in design was able to measure the throat diameter of pores, the largest pore throat diameter, the mean pore diameter, the pore size distribution and permeability of tiny thin walled porous ceramic tubes. Capillary flow porometry successfully measured all these properties. Mercury intrusion technique was incapable of measuring many of these properties.

INTRODUCTION

Ceramic membranes have potential for applications as critical components in many industries because of their inert, strong, reusable and temperature resistant capabilities. Innovative processing techniques have been successfully developed to manufacture thin wall porous ceramic components including tubes of diameter down to a few microns. The performance of the components is determined by their pore size and pore distributions. A novel technique has been developed to measure diameters of very small pores of tiny tubular membranes having very low permeability. The technique is capable of measuring the diameter of the pore's most constricted part, which acts as the barrier. The largest pore throat diameter, the mean pore diameter, the pore size distribution and permeability are also measured. In this paper, the results of the investigation of the pore structure characteristic of micro tubular ceramic membranes manufactured using an innovative technique are presented.

EXPERIMENTAL

Material

Thin wall ceramic micro tubular alumina and composite (two oxides) membranes were investigated. The processing of these materials was based on electrophoretic deposition (EPD). Electrophoresis is the motion of charged particles in a suspension under the influence of an electric field [1]. First application of EPD process for deposition of ThO_2 and tungsten on platinum cathode was made in 1933 [2]. The process was further developed at the Alberta research council, Canada for the manufacture of the ceramic tubes. The tubes were about 3 to 0.1 mm in diameter and >150 mm in length. The cross-section of one such micro tubular alumina membrane is shown in Figure 1. This tube is about 1.3 mm in diameter and 0.1 mm in wall thickness.

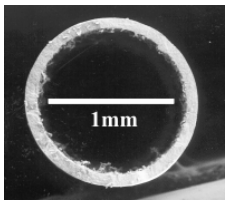

Figure 1. Cross-section of a typical porous alumina tube used in this investigation.

The SEM picture of the cross-section of an alumina tube is shown in Figure 2(a). The tube wall shows granular structure and considerable intergranular porosity. The structure of the composite tube is shown in Figure 2(b). The composite also shows considerable porosity.

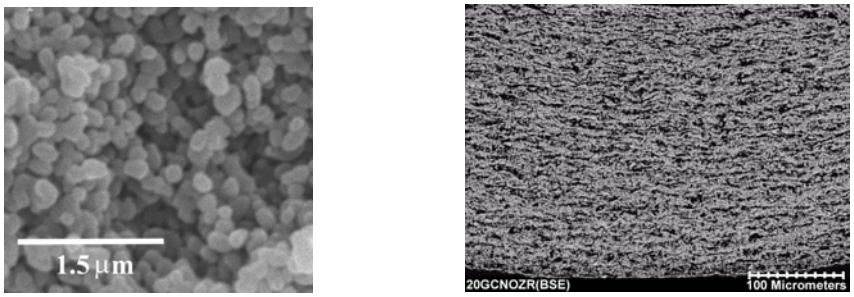

(a) **(b)**

Figure 2. SEM structure. (a) Alumina tube. (b) Composite tube.

A sintered ceramic membrane may be normally expected to contain closed pores, blind pores and through pores (open pores). Closed pores are not accessible. Blind pores do not permit flow. But only the through pores determine the barrier characteristics and permeability of the membrane. Capillary flow porometry was used to evaluate the through pore structure of the ceramic micro tubular membranes.

Capillary Flow Porometry

Principle: The pores of the material to be tested are filled with a liquid whose surface free energy with the sample is lower than the surface free energy of the sample with a non-reacting gas. Such a liquid is known as the wetting liquid. The wetting liquid spontaneously fills the pores. The liquid, which cannot spontaneously come out of pores, is forced out by increasing pressure of the non-reacting gas on one side of the sample. The pores from which liquid is removed permit gas to flow (Figure 3).

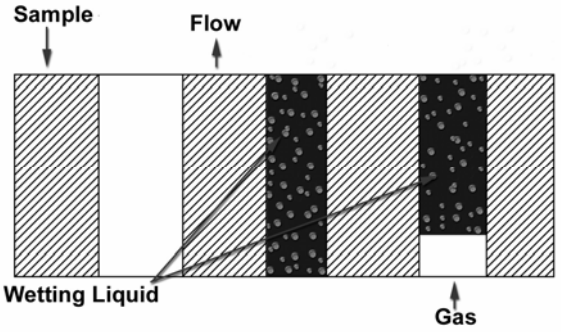

Figure 3. Principle of capillary flow porometry

The pressure required to displace the wetting liquid from a pore is given by the following relation obtained by free energy balance [3]:

$$p = 4 \gamma \cos \theta / D \quad (1)$$

where, p is the differential pressure across the pore, γ is the surface tension of the wetting liquid, θ is the contact angle of the wetting liquid and D is the pore diameter. Pore diameter at any desired location in the pore path is defined as the diameter D, of a cylindrical opening such that (dS/dV) of the pore is the same as the (dS/dV) of the cylindrical opening. Where S is gas/solid surface area and V is the volume of the gas in the pore [3]. For small surface tension wetting liquids, the contact angle may be taken as zero [4].

The measured pressure of gas and flow rates of gas through dry and wet samples yield many properties including constricted pore diameters, the largest pore diameter, the mean flow pore diameter, the flow distribution and gas permeability [5].

Instrument: The sample chamber of the instrument had a unique design to hold tiny samples of the tube. The pores of the sample were filled with the wetting liquid galwick™. The surface tension of galwick was 16 mJ/m^2. The low vapor pressure of the liquid prevented errors due to evaporation. Dry air was used as the gas. The instrument was designed for use at high pressures required for the small pores in the sample. Although, gas flow rates through the tiny samples were very low, the instrument had the capability to measure low flow rates accurately. Test execution, data acquisition, data storage and data reduction operations were fully automated in order to obtain objective results. The instrument was capable of giving reliable and accurate data [5]. The PMI capillary flow porometer used in this investigation is shown in Figure 4.

Figure 4. The PMI capillary flow porometer with capability to measure gas and liquid flow rates.

RESULTS AND DISCUSSION

Throat Diameters of Through Pores

The gas pressure and flow rates through an alumina tube of diameter 2.93 mm and thickness 0.026 mm are shown in Figure 5. In this figure, dry curve and wet curve represent measured flow rates as functions of pressure through dry and wet samples respectively. Half-dry curve is derived from the dry curve to yield half of the flow rate through dry sample at any pressure. The measured differential pressures are used to compute pore diameter after Equation 1.

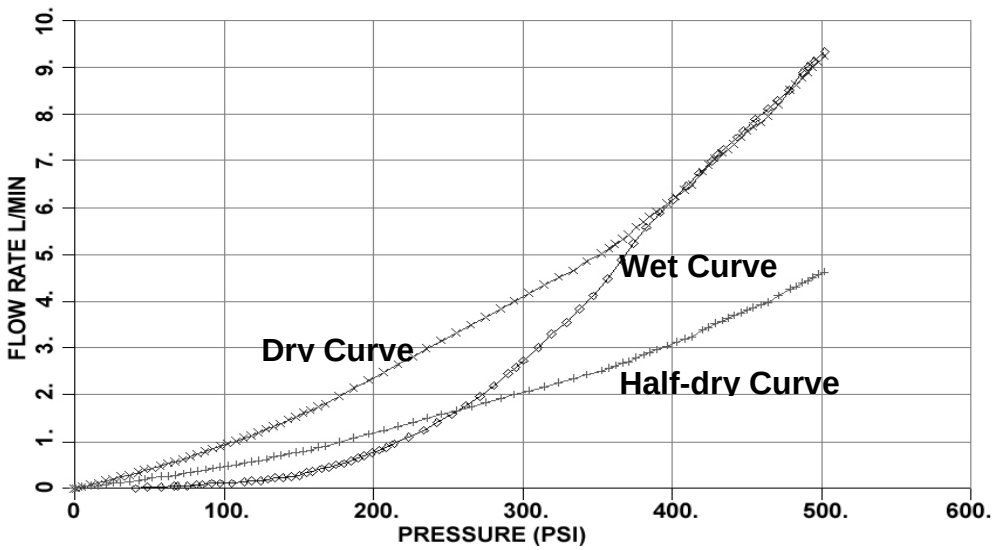

Figure 5. Flow rates through an alumina tube measured as functions of differential pressure in the capillary flow porometer.

The pore diameter normally varies along the pore path because the cross-section tends to change along the pore length (Figure 6). When differential gas pressure is increased on a pore filled with a wetting liquid, the gas tends to remove liquid from the pore and flows through the pore. Equation 1 suggests that low pressure is required to displace liquid in the wide part of a pore. Increasing pressure will displace liquid from parts of the pore of decreasing size (Figure 6). When pressure sufficient to displace liquid from the most constricted part of the pore is reached, gas removes the rest of the liquid from the pore and flows through the pore. Capillary flow porometry detects pores by noting the increase in flow rate at a given pressure, because of removal of liquid from the pores at that pressure. Therefore, the pore size computed from the pressure is the size of the pore at its most constricted part. The diameters of through pores at their most constricted parts govern the flow and barrier properties of the tubular membrane. Such pore diameters are measured by capillary flow porometry

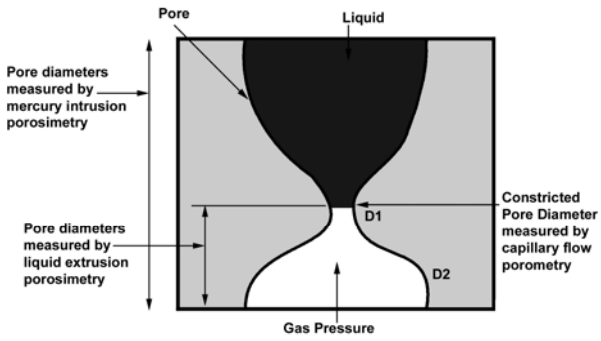

Figure 6. The most constricted pore diameter measured by capillary flow porometry. Diameters measured by porosimetry are also shown for comparison.

The Largest Pore Diameter: The largest constricted diameter of the through pores is obtained from the pressure needed to initiate flow through a wet sample. The instrument employs a special technique to detect the initiation of flow accurately. The largest pore diameter computed from data in Figure 5 is 164 nm in the alumina tube. The largest pore diameters of the composite are 487 nm. The results are listed in Table 1.

Table 1. Pore diameters

Tube	Dimensions, mm		Pore diameter, nm		
	Diameter	Thickness	Largest	Mean	Range
Alumina Tube	2.9	0.026	164	25.6	16 - 164
Composite Tube	2.5	0.451	487	237	41 - 487

Mean Flow Pore Diameter: The mean flow pore diameter is computed from the mean flow pressure, which is the pressure at which wet flow is the same as the half-dry flow. Pores smaller than the mean flow pore permit fifty percent of the flow and the other fifty percent of the flow is through pores larger than the mean flow pore. The mean flow pore diameter is a measure of liquid and gas permeability [5]. The mean flow pore of the alumina tube obtained from data in Figure 5 is 25.6 nm. The mean flow pore diameter of the composite tube is much larger (Table 1).

Pore Diameter Range The largest measured pore diameter is obtained from the pressure at which flow is initiated. The smallest pore diameter is computed from the pressure at which the wet and dry curves meet. The results for the two investigated membranes are listed in Table 1.

Flow Distribution Over Pore Distribution

Pore distribution is defined in terms of the distribution function, f.

$$f = - d [(f_w/f_d)\times 100] /d D \quad (2)$$

where f_w and f_d are the flow rates through wet and dry samples at the same differential pressure. The distribution in the alumina tube computed from data in Figure 5 is shown in Figure 7. The area under the distribution function in a given pore size range yields percentage of flow through pores in that specified range. The tube shows a sharp unimodal distribution. Although, the pore diameters are in the range of 16 – 164 nm, pores are appreciable only in the range of about 16 to 60 nm.

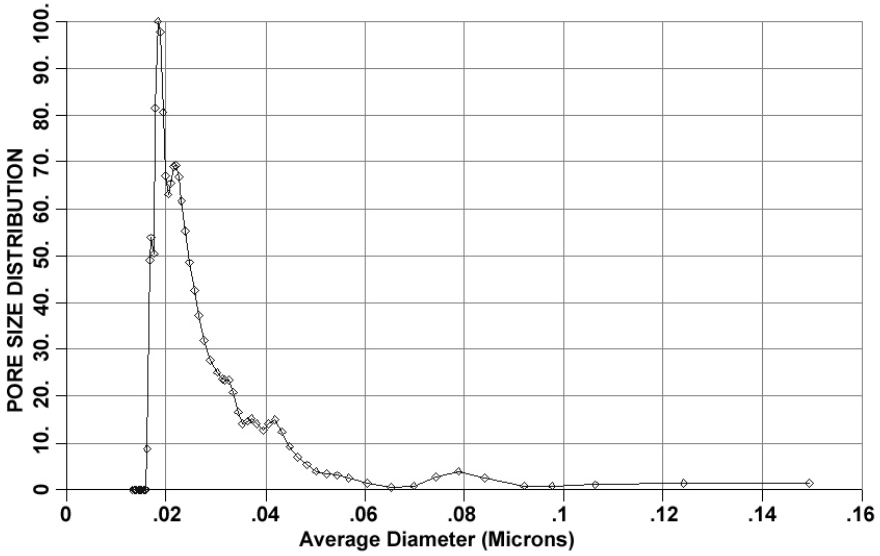

Figure 7. Pore distribution in alumina tube.

The distribution of pores in the composite tube is shown in Figure 8. The pores are in the range of about 41 to 487 nm. However, most of the pores are in the range 50 to 250 nm. Thus, the distribution in the composite tube is unimodal, but much broader than that in the alumina tube.

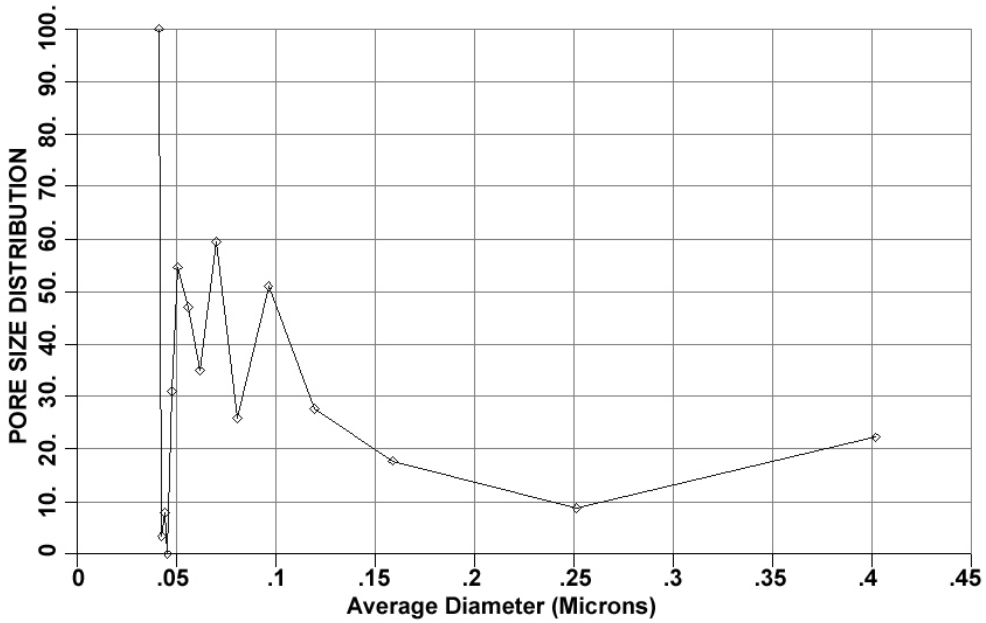

Figure 8. Pore distribution in composite tube.

Permeability

The permeability, k, is defined by Darcy's law [6].

$$\underline{F} = k\,[A/(\mu l)]\,p \qquad (6)$$

where, $\underline{F}$ is the flow rate in volume at average pressure, k is permeability, A is the area of the sample, l is the thickness of the sample, μ is the viscosity of fluid and p is the differential pressure across the sample.

Gas Permeability: The flow rate measured through dry sample (Figure 5) is used to calculate gas permeability of the sample. The instrument has unique ability to measure gas permeability as a function of pressure. Permeability may be computed in any desired unit such as Darcy, Frazier, Gurley and Rayle. The air permeability of the alumina tube (Figure 5) is 3.7×10^{-6} Darcies. The air permeability of the composite is 9.96×10^{-3} Darcies. The pressure dependence of permeability is demonstrated by the variation of airflow rate through the sample as a function of pressure (Figure 9) up to 180 psi.

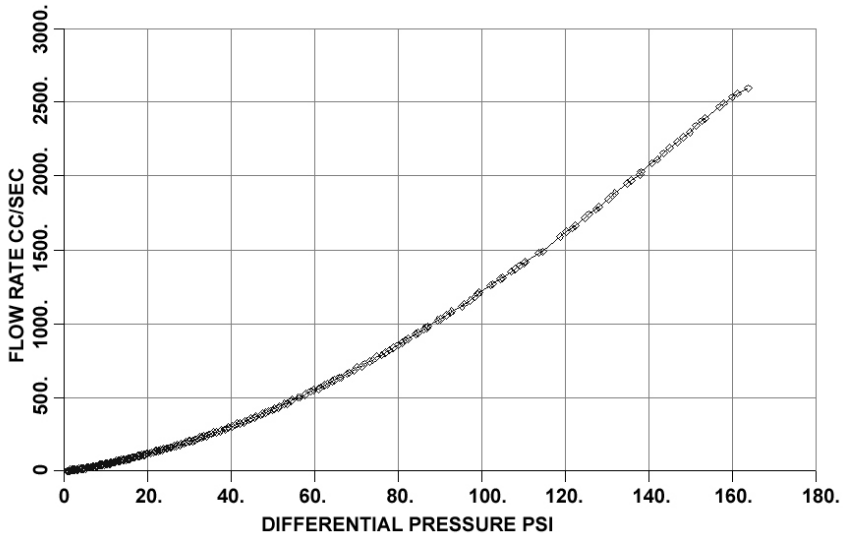

Figure 9. Variation of airflow rate through the composite tube as a function of pressure.

Liquid Permeability: The capillary flow porometer has the required feature to measure flow rate of liquid as a function of differential pressure for evaluation of liquid permeability. Permeability of an alumina tube for water measured in the capillary flow porometer was 134×10^{-6} Darcies.

Comparison with Other Techniques

Mercury porosimetry is often used for pore structure analysis. In this technique mercury under pressure is forced into pores of the sample. Pressure gives pore diameter and intrusion volume gives pore volume and pore volume distribution. This technique gives total pore volume of through and blind pores. However, constricted pore diameter and the largest pore diameter are not measurable. Because the pore diameter is based on volume, each pore is measured as several pores and the wider parts of pores lead to a shift of pore distribution to larger pore sizes (Figure 6). The pore distribution by mercury porosimetry is not as sharp as that determined by flow porometry [7]. Both gas and liquid permeabilities are not measurable by mercury porosimetry. Also this technique uses mercury, which is toxic and the pressures required are very high. Table 2 lists features of the two techniques.

Table 2. Comparison of capillary flow porometry with mercury intrusion porosimetry.

Capability	Capillary Flow Porometry	Mercury Intrusion Porosimetry
Pore volume	N	Y
Pore volume distribution	N	Y
Constricted pore diameter	Y	N
Largest pore diameter	Y	N
Mean flow pore diameter	Y	N
Flow distribution	Y	N
Gas permeability	Y	N
Liquid permeability	Y	N
Avoidance of toxic material	Y	N
Avoidance of high pressure	Y	N
High temperature tests	Y	N
Tests in strong chemical environments	Y	N

SUMMARY AND CONCLUSION

1. Tubular membranes with diameter in the range of about 3 mm to < 0.1 mm, thickness of several tenth of a millimeter and length of several centimeters were successfully manufactured using the EPD process.
2. Capillary flow porometry was modified to characterize pore structure of the tiny tubular membranes. Several alumina tubes and a composite tube were investigated.
3. The alumina membrane had 164 nm largest pore diameters, 25.6 nm mean flow pore diameters, 16 – 164 nm pore diameter range, 3.7×10^{-6} Darcies air permeability and 134×10^{-6} Darcies water permeability. Flow distribution through the alumina tube over pore diameter was also measured.
4. The composite membrane had 487 nm the largest pore diameters, 237 nm mean flow pore diameters, 41 - 487 nm pore diameter range and 9.96×10^{-3} Darcies air permeability. Flow distribution through the composite tube over pore diameter was also computed
5. This investigation showed that capillary flow porometry is capable of measuring pore characteristics of the tiny tubular membranes containing very small pores. Mercury porosimetry is incapable of measuring all of these properties.

REFERENCES

[1]W.F. Pickard, J. Electrochemical Soc., 115 (1968), 105C-108C.
[2]E. Harsanyi, U.S. Patent No. 1897902, 1933.
[3]A. K. Jena and K. M. Gupta, Journal of Power Sources, 80 (1999), 46.
[4]Vibhor Gupta and A. K. Jena, Advances in Filtration and Separation Technology, American Filtration & Separation Society, 13b (1999), 833.
[5]A. Jena and K. Gupta, F &S Filtrieren und Separieren, 16 (2002), 13.
[6]P.C. Carman, Flow of Gases through Porous Media, Academic press, 1956.
[7]Akshaya Jena, Howard Sanders, Jamie Miller and Rick Wimberly, IEEE 01TH8533 (2001) 71.